Construction and Building Materials 225 (2019) 340–347

Contents lists available at ScienceDirect

Construction and Building Materials

journal homepage: www.elsevier.com/locate/conbuildmat

Instantaneous monitoring the early age properties of cementitious materials using PZT-based electromechanical impedance (EMI) technique

Yen-Fang Su [a], Guangshuai Han [a], Adlan Amran [a], Tommy Nantung [b], Na Lu [a,c,d,*]

[a] Lyles School of Civil Engineering, Sustainable Materials and Renewable Technology (SMART) Lab, Purdue University, 550 Stadium Mall Drive, West Lafayette, IN 47907-2051, USA
[b] Office of Research and Development, Indiana Department of Transportation, USA
[c] School of Materials Engineering, Purdue University, USA
[d] Birck Nanotechnology Center, Purdue University, USA

HIGHLIGHTS

- The comprehensive study of using PZT based EMI method to monitor the properties of cement mortar.
- Experiments were conducted on mortar with various w/c ratio on different cements.
- RMSD is the most efficient index to reflect the stiffness growth of cement mortar.
- The EMI-RMSD index might be independent from the various w/c ratio of cement mortar.

ARTICLE INFO

Article history:
Received 13 March 2019
Received in revised form 11 May 2019
Accepted 17 July 2019

Keywords:
Electromechanical impedance (EMI)
Early age property
Very early age property
Cementitious materials
Compressive strength
Piezoelectric materials

ABSTRACT

The use of piezoelectric materials based Electromechanical Impedance (EMI) technique for monitoring the hydration of cementitious materials has caught much attention recently. However, very few literatures have explored the feasibility of using this method on monitoring the stiffness development and compressive strength gain at the very early age properties (4th–8th h) of cementitious materials. This research serves as a comprehensive study to verify the reliability of using lead zirconate titanate (PZT) based EMI method in monitoring the compressive strength gain and elastic modulus of mortar at both very early age (4th–8th h) and early age (1st, 3rd, and 7th day). Extensive experiments and data analysis have been done on ten different mixes with various water-to-cement ratio and Type I & III cement. The EMI signatures are measured for each sample at the period of interest, and post-processed with three statistic model including the root mean square deviation (RMSD), correlation coefficient deviation (CCD), and mean absolute percentage deviation (MAPD) as indices. To examine the correlation and linearity between the compressive strength/elastic modulus obtained via conventional cubic testing using ASTM C109 and the EMI indices, a linear least square regression analysis is performed. As the authors postulated, all the mixes display a good linear correlation of R^2. Among all three statistical indices, RMSD index is proved as the most accurate statistical index on strength gain monitoring of cementitious materials. The results indicated the feasibility of using piezoelectric-based EMI method for monitoring the cementitious material's strength gain at very early age, regardless the concrete mix design.

1. Introduction

It is critical to develop accurate and reliable nondestructive testing (NDT) methods for in-situ monitoring the strength gain of cementitious materials at very early and early age, due to fast-paced construction schedule, particularly airport or highway overlay paving projects. Nevertheless, the conventional destructive testing methods such as compressive test and flexural test are very time consuming, moreover, the curing condition of the tested samples and in-situ condition are quite different. An NDT method which can directly correlate with the mechanical properties of cementitious materials regardless the curing condition, mix design, size effect is needed for in-situ application.

* Corresponding author.
E-mail addresses: luna@purdue.edu (Y.-F. Su), luna@purdue.edu (N. Lu).

https://doi.org/10.1016/j.conbuildmat.2019.07.164
0950-0618/

Piezoelectric materials based electromechanical impedance (EMI) technique have shown promised in addressing this challenge, as it has been used for both properties monitoring and damage detection of the concrete structure. Due to the direct and inverse piezoelectric effect, piezoelectric materials can act as sensor, actuator and transducer [1–3]. Among them, the piezoceramic material- PZT (lead zirconate titanate), has been heavily used as a sensor due to its outstanding piezoelectric proprieties such as high charge constant and sensitivity, fast response, long-term stability and low-cost [4].

Soh and Bhalla [5] made the first attempt to use EMI method on detecting the strength of concrete. Their proposed an empirical fuzzy probabilistic damage model to quantify the damage condition of concrete. Shin et al. [6] extended the EMI sensing technique from damage detection of concrete to material properties monitoring. They tracked the concrete strength gain at the age between 3 and 28 days. It was found that the EMI signature shifts from left to right as the time increases due to the hydration process change the mechanical properties of concrete. Tawie et al [7] has demonstrated the EMI technique for concrete strength monitoring on high water-to-cement ratios concrete and has discovered that the EMI result shown an exponential increment in the frequency shift at the age from 3rd to 28th day from their curve fitting result. Wang et al [8] designed the asphalt lacquer coated PZT sensor for the concrete strength monitoring. The testing age is from the first day till 28 days after the concrete cast. They concluded that the post statistic treatment of real admittance can better reflect the compression gain of concrete than the imaginary admittance. Lu et al [9] proposed a PZT based sensor called "Smart Probe" to improve the efficiency of monitoring the concrete properties. The Smart Probe was made by aluminum beam with the PZT bonded on the surface, and partially embedded into concrete for measurement. The experimental results exhibited that the resonance peak at the frequency range from 5 k to 30 kHz of sensor can efficiently monitor the strength gain of mortar. Gafari et al [1] evaluated the compressive strength gain of cement paste with different supplementary cementitious materials (SCMs) including fly ash and silica fume. The results presented the feasibility of utilizing EMI-RMSD index on monitoring strength gain progress for the cementitious materials incorporated with SCMs at the age from 1 day to 28 days. Negi et al [10] discussed the efficiency of embedded orientation of PZT sensor in concrete. They concluded that the inclined orientation (45°) is the least efficient compared with the horizontal and vertical placed (0° and 90°).

Up to now, using PZT based EMI method on concrete strength monitoring from 1 day to 28 days has been well studied. Nevertheless, there's very limited research conducted on understanding the EMI methods for in-situ monitoring of the very early age properties of cementitious materials. Tawie et al [11] bonded the PZT sensor on the steel bar in the reinforced concrete (RC) to monitor the bonding properties between concrete and rebar at the age from 1 h to 168 h after casting. The frequency shift (%) of the conductance spectrum was accessed as the index to quantify the bonding condition. The results revealed that the frequency shift index will affect by the vary of w/c ratio and curing temperature. Kong et al [12] fabricated a sandwich structural PZT transducer (called smart aggregate) to characterize the concrete hydration at very early age (0–20 h). The signal response from the sinusoid wave with the constant frequency of 90 kHz and 100 kHz can successfully differentiate the three stage of concrete hydration. Providakis et al.[13] proposed the reusable Teflon-based PZT transducer to monitor the early-age concrete hydration process. The sensor was bonded on the top of concrete sample and connect with the low-cost system-on-chip impedance spectrometer –AD5933, which have the potential for wireless sensing. Depend on their experiment outcome, the modified RMSD index decreased with the time elapsed after 9 and 12 h after concrete casting. Narayanan et al.[14] embedded the multi-layer protection PZT sensor into the cement mortar to track the impedance change of materials. Using EMI signature, they have analyzed several early age properties including setting time, Young's modulus and isothermal calorimetry measurement. It has concluded that the magnitude changes in the impedance of PZT and shift of frequency can be reflected as the changes of the stiffness of the cement mortar. Visalakshi et al. [15] also bonded the PZT sensor on the rebar and embedded into concrete to monitor the concrete hydration. They proposed a hydration index (h) which comprise of stiffness concept extracted from the admittance signature to monitor the hydration of concrete. The hydration parameter increased with the sample aged, which means it can capture the evolution of hydration of concrete. Table 1 summarizes the studies of hydration related monitoring of cementitious materials via EMI technique so far.

As shown in Table 1, none of the existing research have directly used the EMI signature to study the compressive strength gain and development of elastic modulus for the cementitious materials at the very early age (4–8 h). More importantly, the effect of different mix design on the reliability of EMI methods have not been investigated in existing literature.

Table 1
Literature of applying EMI method for hydration monitoring of cementitious material.

Reference	Materials	Dimension/Configuration of PZT	Sample (Testing) age
2008, Shin et al [6]	Concrete	$10 \times 10 \times 0.2$ mm/surface bonded	3,5,7,14,28 days
2010, Tawie et al [7]	Concrete	$10 \times 10 \times 0.5$ mm/surface bonded	3,7,14,28 days
2010, Tawie et al [11]	Concrete	$10 \times 10 \times 0.3$ mm/embedded-bonded on steel bar	1,3,6,9,12,24,72,168 h
2010, Annamdas et al [16]	Concrete	$10 \times 10 \times 0.2$ mm/embedded-epoxy wrapped	2,5,8,15,26,31 days
2011, Wang et al [8]	Concrete	$8 \times 8 \times 0.3$ mm/embedded-Asphalt Lacquer coated	1,2,3,4,7,14,21,28 days
2013, Kim et al [17]	High strength concrete	$20 \times 20 \times 0.5$ mm/surface bonded	3,5,7,14,21,28 days
2013, Kong et al [12,18]	Concrete	$15 \times 15 \times 0.3$ mm/embedded-sandwich with two marble blocks	0–20 h
2013, Providakis et al [19]	Concrete	$10 \times 10 \times 0.2$ mm/partially embedded- Teflon-based enclosure	3,6,9,12,15,18,21,24 h –28 days
2014, Wang et al [20]	Concrete	$8 \times 8 \times 0.3$ mm/embedded-Asphalt Lacquer coated	1,2,3,4,7,14,21,28 days
2017, Narayanan et al [21]	Mortar	$20 \times 20 \times 1$ mm/embedded -thermosetting epoxy coated	1,8,16 h, 2,5,12,16,20,22,25,28 days
2017, Lu et al [9]	Concrete	$10 \times 10 \times 0.3$ mm/partially embedded-surfaced bonded on the aluminum plate	1,2,3,7,14,28 days
2018, Gafari et al [1]	Cement paste (SCMs)	$10 \times 10 \times 0.2$ mm/surface bonded	1,3,7,14,28 days
2018, Negi et al [10]	RC	$10 \times 10 \times 0.3$ mm/embedded-bonded on cement block	3,7,14,21,25,28 days
2018, Visalakshi et al [22]	Concrete	$10 \times 10 \times 0.3$ mm/embedded-bonded on steel bar	1–12 h, 1–28 days

To this end, the aim of this study is to investigate the feasibility of using EMI method for monitoring the compressive strength gain process of cementitious materials from very early age (4th–8th h) to the early age (1st to 7th day) with various mxi design. The EMI signatures are recorded using surface bonded PZT sensor with compressive test conducted simultaneously. The mechanical compressive test results are further correlated with EMI signatures which post-processed via different statistic techniques such as root mean square deviation (RMSD), correlation coefficient deviation (CCD), and mean absolute percentage deviation (MAPD).

A linear least square regression (R^2) is utilized to determine the correlation coefficients between each index of the EMI signatures and the mechanical compression testing results. Also, the influences of various mixtures with different proportions such as water-to-cement ratio and different type of cement are systematically investigated. Lastly, the feasibility of PZT- based EMI technique for monitoring the concrete at the very early age is established.

2. Experimental program

2.1. Materials

Type I (ordinary) and type III (high early strength) Portland cements are both used as the binder of 50 mm cubic specimen. The W/C ratio range varied from 0.38 to 0.46 with the increment of 0.02. Mortar is prepared by adding fine graded Ottawa test sand according to the ASTM C150 and ASTM C778 standards. The cement-to-sand ratio of various mix designs are kept at 1:3. All 10 sets of the mix in this study are tested at the very early age (4th–8th after blended water with cement) and the early age (1, 3, 7 days). In order to minimize the variables, the EMI test and mechanical test are performed at the exact same time during each age. The samples are stored in standard moisture curing room at the temperature of 23 ± 2 °C until the test age.

2.2. Testing

2.2.1. EMI test

In the EMI test, the host sample of each mix is surface mounted by a $10 \times 10 \times 0.2\ mm^3$ PZT patch with a fast-set epoxy (5 minus set, cured in 1 h) as the binding agent. Each PZT patch is connected to two wires using cold silver soldering to prevent burning of the sensor. These two wires are attached to an impedance analyzer which is linked to a computer equipped with a data acquisition software (Fig. 1). The EMI test started at 4th hour as baseline and the signals are taken from 5th–8th h with a 1-hour interval. Same procedures are also conducted at 1st, 3rd, and 7th day.

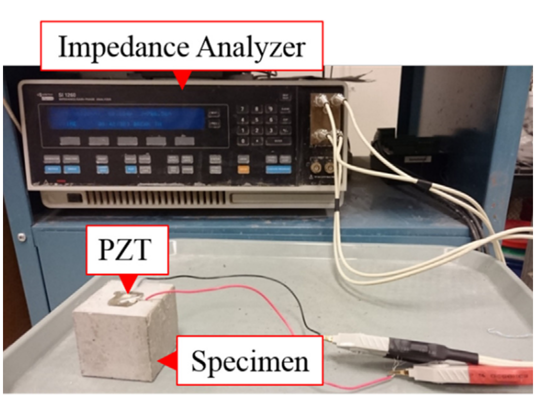

Fig. 1. EMI test setup.

2.2.2. EMI signal

An EMI signature is dependent on a direct and inverse piezoelectric effect of a piezoelectric material. During an EMI test, the impedance analyzer discharges a sinusoidal AC voltage (500 mV) to excite a bonded PZT patch with a high-frequency range between 100 kHz and 500 kHz with the reasonable resolution of 10 kHz. The analyzer then records the response of the PZT's electromechanical dynamic impedance. The mechanical impedance of the host structure (Z_s) and that of PZT sensor (Z_a) can induce an electrical impedance of PZT which is the reciprocal of admittance (Y). The admittance response is governed by the PZT's theoretical admittance model shown below model [23]:

$$Y = G + Bj = 4\omega \frac{l^2}{h}\left[\overline{\varepsilon_{33}^T} - \frac{2d_{31}^2 Y^E}{(1-\upsilon)} + \frac{2d_{31}^2 \overline{Y^E}}{(1-\upsilon)}\left(\frac{Z_a}{Z_a + Z_s}\right)\frac{\tan kl}{kl}\right] \quad (1)$$

where the admittance is a function of conductance (G), susceptance (B) with its imaginary unit (j), PZT sensor dimension (w, l, and h – width, length, and height), electrical permittivity ($\overline{\varepsilon_{33}^T} = \varepsilon_{33}^T(1-\delta j)$), piezoelectric coefficient (d_{31}), dynamic young's Modulus ($\overline{Y^E} = Y^E(1+\eta j)$), Poisson's ratio ($\upsilon$), and wavenumber ($k$). Except for Y, G, Z_a, and Z_s, all variables are a material property.

2.2.3. Statistical methods for signal processing

For each sample, the conductance signature is further quantified by referencing the baseline signature via the three different statistical models including root mean square deviation (RMSD), correlation coefficient deviation (CCD), and mean absolute percentage deviation (MAPD). The equation is shown below:

$$RMSD\,(\%) = \sqrt{\frac{\sum_{i=1}^{N}(G_i - G_{bl})^2}{\sum_{i=1}^{N}(G_{bl})^2}} \quad (2)$$

$$CCD(\%) = 100 - \left\{\frac{1}{N\sigma_{G_i}\sigma_{G_{bl}}}\sum_{i=1}^{N}[(G_i - \overline{G_i})\cdot(G_{bl} - \overline{G_{bl}})]\right\} \quad (3)$$

$$MAPD(\%) = \frac{1}{N}\sum_{i=1}^{N}\left|\frac{(G_i - G_{bl})}{G_{bl}}\right| \quad (4)$$

where G_i is the spectra of different curing age, G_{bl} is the baseline spectra obtained at the 4th hour of curing, N signify the number of data points in the EMI spectra, σ and $\overline{G}$ stand for the standard deviation and the mean, respectively.

2.2.4. Setting time measurement

Setting time for each mix are evaluated by an automatic VICAT needle device. The test is based on standard ASTM C807 and ASTM C191. Based on the standard, the needle drops in the mortar sample every 10 min until the penetration reach 25 mm. The first setting is determined as the elapsed time required to achieve a penetration of 25 mm. The purpose of measuring setting time is to determine whether the mortar specimen is stiffening enough to demold and to surface bond the PZT sensor on the sample.

2.2.5. Compressive test

While the EMI test runs, conventional compressive tests are conducted on three identical specimens of each mix according to the ASTM C109. The samples are demolded after the initial setting time with dexterity for very early age testing. The test is performed by positioning the sample in a uniaxial load frame. At each curing age of interest, the peak stresses of the three specimens are recorded and averaged. EMI test and compressive test are conducted simultaneously at the curing age of 5th, 6th, 7th, and 8th h and 1st, 3rd, and 7th day. The EMI test at the 4th h determines the baseline for the EMI signature of the subsequent test. In this method, every change in the signature of a sample will be referenced to the baseline signature using the three statistical indices. This is also a way of quantifying the signature change as the sample aged. At each curing age of interest, the signature change from the EMI technique is compared to the data of the compressive test via regression correlation analysis.

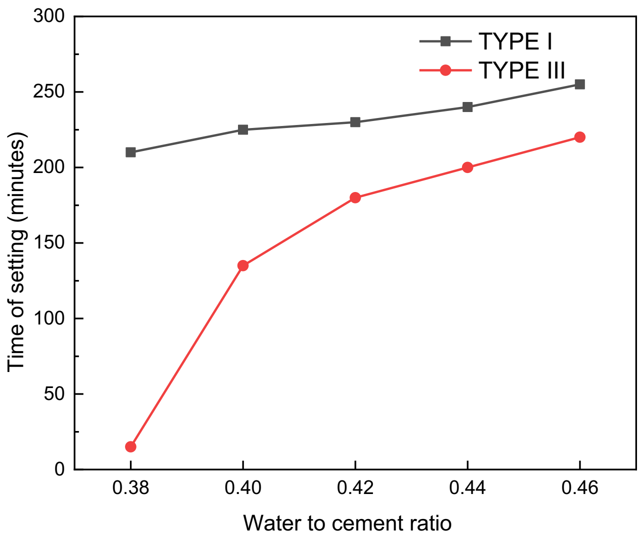

Fig. 2. Initial setting time of type I and type III mortar with various w/c.

3. Experimental result and discussion

3.1. Setting time of different samples

This study comprises a comprehensive investigation of cementitious materials with the various water-to-cement ratio (w/c) and different type of cement. Fig. 2 shows the initial setting time of all samples. It can be seen that setting time increase with the w/c increases. Mortar with type III cement set faster than type I samples. The maximum initial setting time of mortar (i.e. w/c = 0.46) with type I and type III cement is 255 min and 220 min, respectively. The samples have adequate stiffness to demold after 5 h (300 min) to execute the testing.

3.2. Spectrum analysis

The EMI signals of all 10 mixes are measured at each age of interest. Each sample are measured for three times to ensure repeatability. The impedance signal extracts from the analyzer including the real part and the imaginary part. Among two parts, the reciprocal of the real part, in term of conductance, is the most used data to be analyzed due to the explicit changes with the change of the sample conditions, i.e. age, humidity, component of sample [8]. Fig. 3 shows the representative plot of conductance versus frequency of w/c = 0.46 samples with type I and type III cement, respectively. As can be seen that the conductance spectrum shifts from left to right with the age increase. The shift trend of type I mortar is more obvious than that of type III mortar. A rightward shift can also be observed from the result. The reason contributed to the shift of spectrum is the development of the

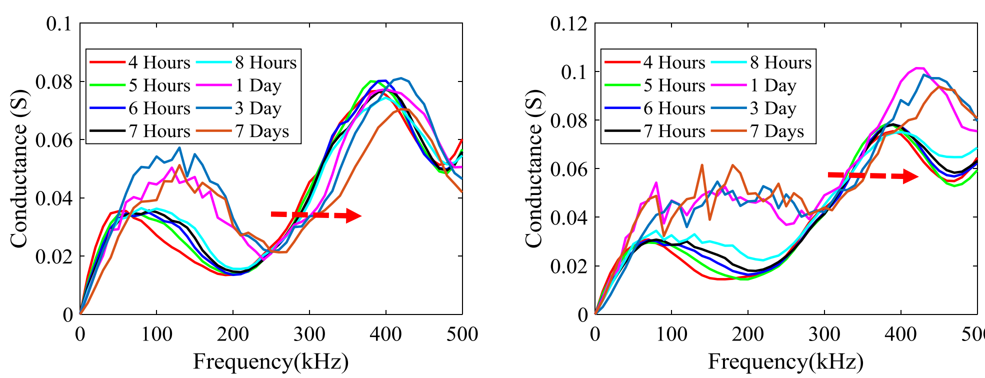

(a) Type I cement mortar, w/c=0.46 (b) Type III cement mortar, w/c=0.46

Fig. 3. Conductance signature of representative sample at different age.

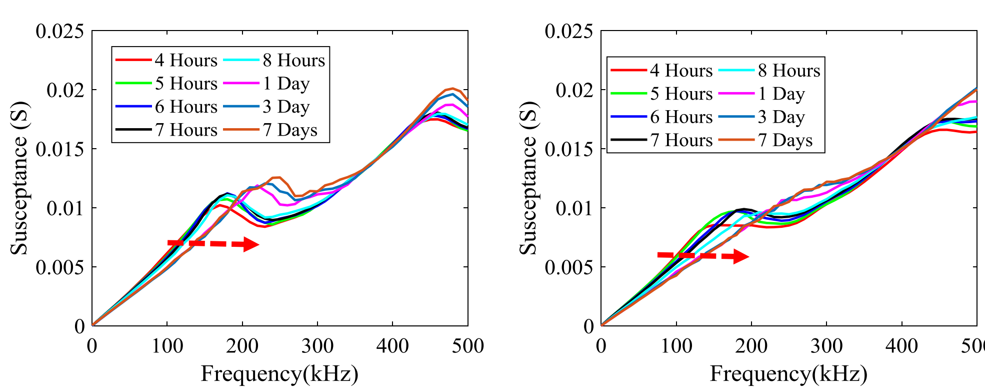

(a) Type I cement mortar, w/c=0.46 (b) Type III cement mortar, w/c=0.46

Fig. 4. Susceptance signature of representative sample at different age.

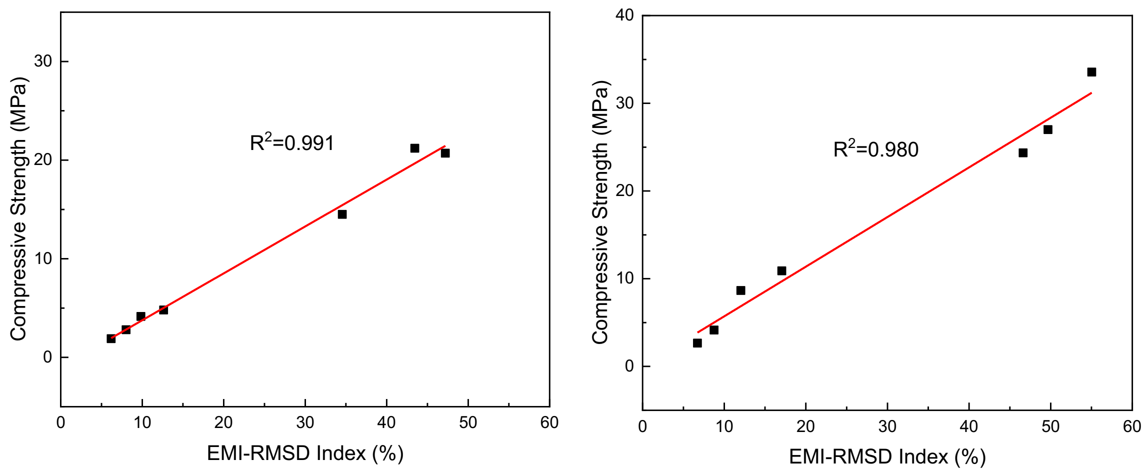

(a) Type I cement mortar, W/C=0.46 (b) Type III cement mortar, W/C=0.46

Fig. 5. The linear correlation fitting between compressive strength with EMI-RMSD index of W/C = 0.46 sample.

stiffness due to the hydration of cement-based material along with age. During the hydration process, the water will either be consumed for the formation of the hydration products such as alite (C_3S), belites (C_2S), and aluminate (C_3A) etc. or evaporated. The stiffness of the sample will increase at this period. The rightward shift of spectrum is reflecting the growth of stiffness.

Table 2
Regression result of compressive test versus EMI-RMSD index.

Mixes:	R^2 (Compression vs. RMSD index)	R^2 (Elastic modulus vs. RMSD index)
Type I, W/C = 0.46	0.991	0.991
Type I, W/C = 0.44	0.997	0.980
Type I, W/C = 0.42	0.989	0.989
Type I, W/C = 0.40	0.980	0.990
Type I, W/C = 0.38	0.988	0.993
Type III, W/C = 0.46	0.980	0.975
Type III, W/C = 0.44	0.958	0.940
Type III, W/C = 0.42	0.986	0.936
Type III, W/C = 0.40	0.940	0.947
Type III, W/C = 0.38	0.968	0.906

Fig. 4 displays the susceptance signature of a representative sample (w/c = 0.46) at different ages. Susceptance is the inverse of the imaginary part of impedance (reactance). We can observe the slope of susceptance spectrum tends to decrease along with the sample aged, and the spectrum are also shift from left to right. The susceptance slope is sensitive to the temperature, and it would change around 1% per 1 °C [24]. Thus, it can be ascribed to the temperature change during the hydration process of cementitious materials [25].

3.3. Statistical methods for signal processing

The post-process statistic matrixes are employed as the quantitative indices to estimate the compressive strength of cementitious materials. RMSD [1,7–10,16,19,22,26–38] is the most used index which provides the superior assessment of concrete strength. To obtain the satisfactory repeatability of the testing, a suitable frequency range selection is very important [39]. Previous study [23] suggested that the frequency range lies between 100 k and 400 kHz would show a better correlation. Thus, the data in this study are processed at the frequency range from 100 k to 400 kHz. Fig. 5 displays the correlation result between RMSD index of the representative sample (W/C = 0.46) with corresponding

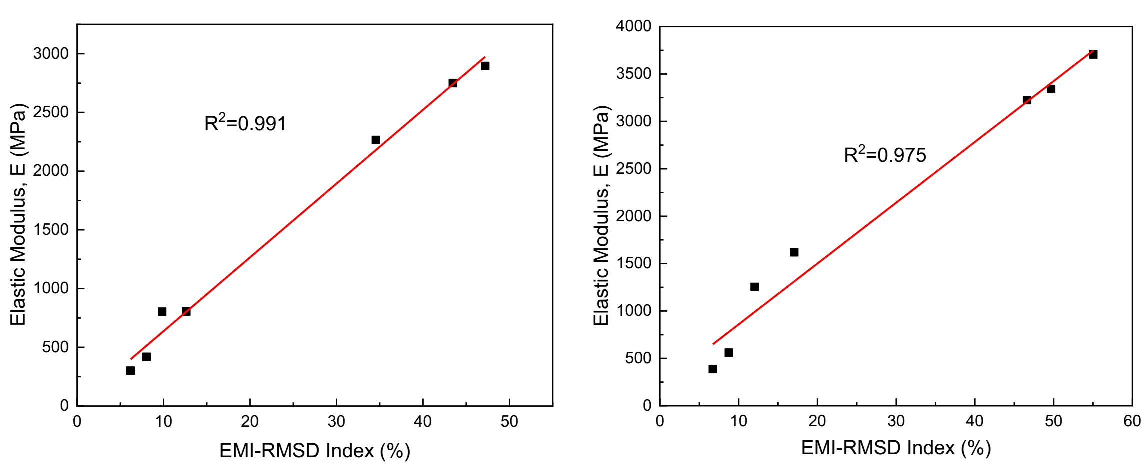

(a) Type I cement mortar, W/C=0.46 (b) Type III cement mortar, W/C=0.46

Fig. 6. The linear correlation fitting between elastic modulus (E) with EMI-RMSD index of W/C = 0.46 sample.

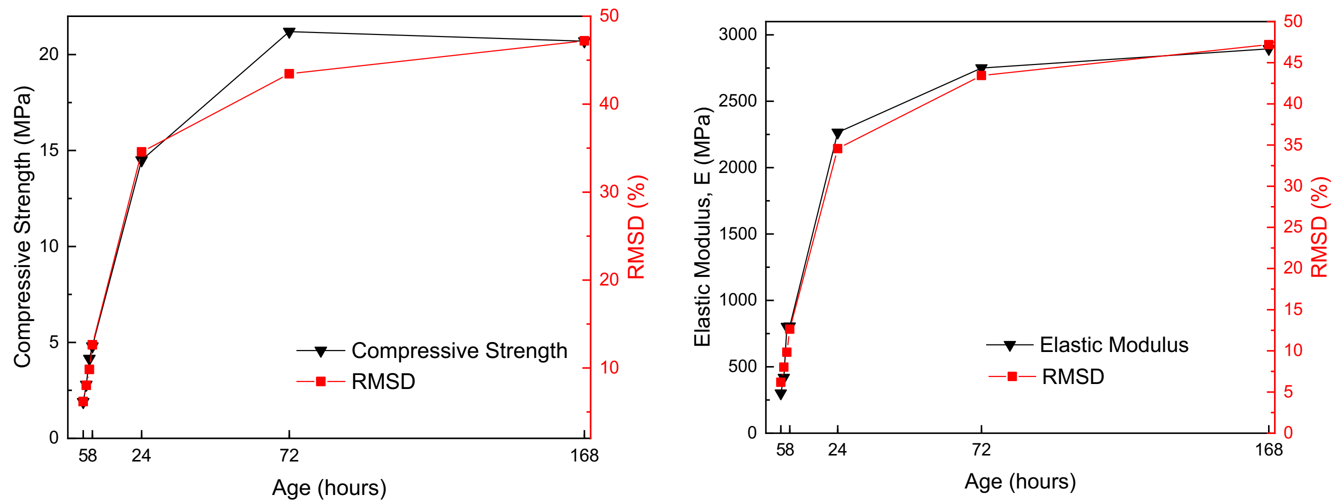

(a) Compression vs. RMSD index

(b) Elasti c modulus vs. RMSD index

Fig. 7. Mechanical properties verse RMSD index of representative sample (Type I, w/c = 0.46) at all ages.

compressive strength at each age. It has been found that the R^2 value is greater than 0.94 for all samples as shown in Table 2. Moreover, the R^2 values of compression for type I samples are higher than 0.98, especially, the value of the samples with w/c of 0.46, 0.44, and 0.42 are greater than 0.99. The elastic modulus is also be recorded and correlated with the RMSD index as Fig. 6 presented. Based on the Hooke's law, compressive strength is linear with elastic modulus, thus, it's not hard to understand that if compressive strength of the samples has high correlation with RMSD index, elastic modulus would perform the same. As Fig. 6 reveals, the R^2 values for the elastic modulus are above 0.97. This signifies that the EMI-RMSD can be used to assess the mechanical properties of cementitious materials with high accuracy.

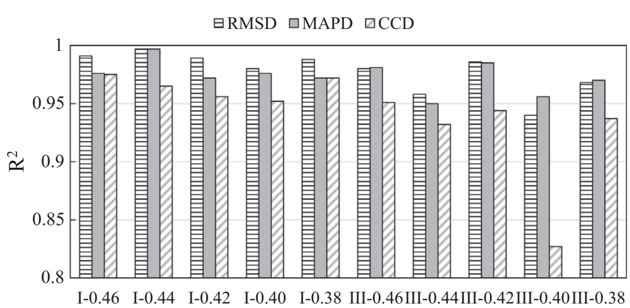

Fig. 8. The correlation value (R^2) of three proposed indices for all mixes.

Fig. 7 exhibits mechanical properties verse RMSD index of a representative sample (Type I, w/c = 0.46) at all ages. The RMSD index tends to increase with the elapse of curing time. Both Fig. 7(a) and (b) display that EMI data have perfectly aligned with that of compressive strength and elastic modulus results, respectively, especially at the very early age. The marginal deviation of 72 h data between compressive testing and EMI method in Fig. 7(a) can be attributed to the inconsistent shape of the compressive testing samples. It can be seen that the RMSD curve fits with elastic modulus data very well in Fig. 7 (b). To sum up, the EMI-RMSD index can accurately reflect the strength growth and stiffness development of cementitious materials.

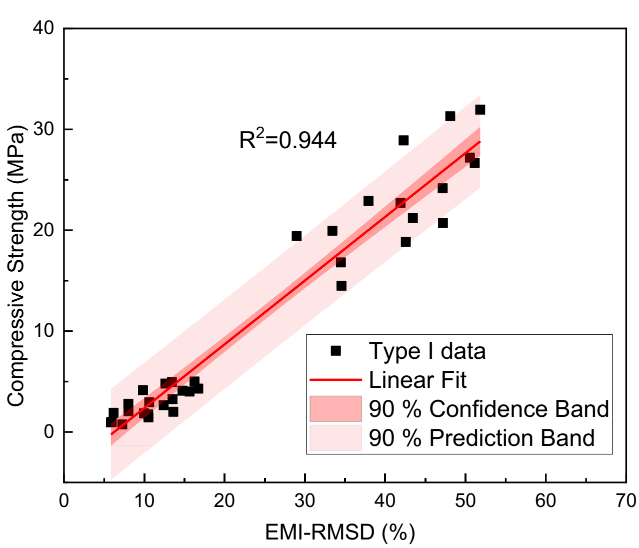

Fig. 9. The correlation between compressive strength and EMI-RMSD of type I cement mortar with different water-to-cement ratio.

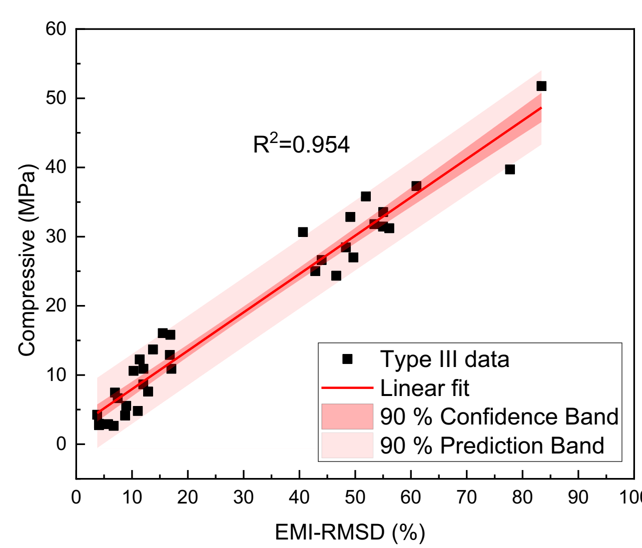

Fig. 10. The correlation between compressive strength and EMI-RMSD of type III cement mortar with different water-to-cement ratio.

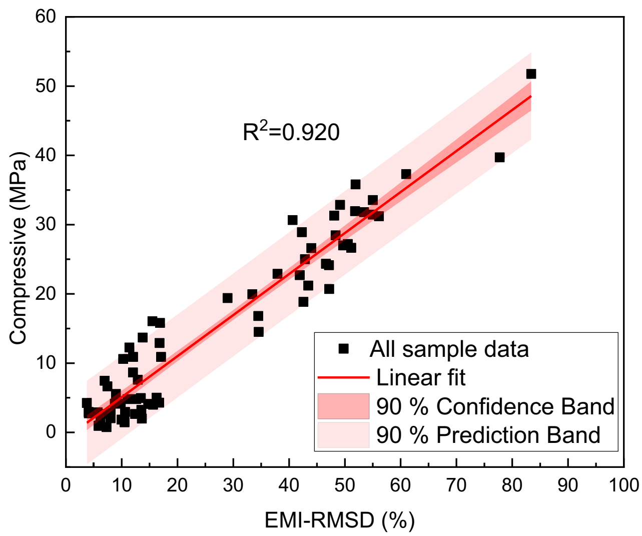

Fig. 11. The correlation between compressive strength and EMI-RMSD of all samples.

The other statistical models including correlation coefficient deviation (CCD) [1,7,20], and mean absolute percentage deviation (MAPD) [7–9,34] are also proposed as a valid index on strength gain monitoring of concrete. In this research, MAPD and CCD index is also being utilized to compare the veracity. From Fig. 8, we can notice that the RMSD has the higher R^2 than that of the others. The MAPD index is also shown acceptable accuracy with the R^2 for all mixes are higher than 0.95. The CCD index is relatively lower compare with others. As can be seen in the figure that the R^2 value is lower than 0.85 for CCD index of type III-0.40 sample.

For the statistical comparison, the data of type I mortar and type III mortar are further lumped as Figs. 9 and 10 show, respectively. The R^2 of lumped type I data is 0.944, and it's 0.954 for type III data, both exhibit the satisfying correlation, which indicated that the EMI-RMSD index might be independent from the w/c. The 90% confidence band and 90% prediction band are further calculated and plot on the figures. Most of the data point of two figure are in the 90% prediction band.

To validate whether the various mix design would affect the correlation, the data from every different mix design is put together for the regression analysis. As can be seen in the Fig. 11, the R^2 drops to 0.92, and the prediction band is broader than Figs. 9 and 10. This can be attributed to the slight differences of each sensor and the bonding process. Although the sensor being used in this study are fabricated and bonding followed the same standard operation procedure, the slightly variation is unavoidable.

4. Conclusion

This research presents a comprehensive study on a very early age (4th–8th h) and early age (1st, 3rd, and 7th day) strength monitoring of cementitious materials using PZT based EMI technique. Ten sets of mortar sample with five different w/c and two types of cement are tested for both EMI test and compressive test (ASTM C109). The impedance spectrum is analyzed and discussed. The statistics models including RMSD, MAPD, and CCD are also utilized to post-process the EMI signature. To verify the reliability of the index, the regression analysis has been employed. Three different indices exhibited reasonable correlation with compressive strength gain and elastic modulus of mortar samples.

Among the statistical indices, RMSD is found to be the most accurate one, which the R^2 value of the type I mortar with w/c of 0.46, 0.44, and 0.42 are greater than 0.99. The MAPD index displayed the R^2 above 0.95 for all mixes is also considered a satisfied index.

Some literature suggested that the relationship between concrete properties and the indices should be exponentially correlated [40]. However, the extensive experimental result obtained from this study indicated that the relationship of early age (including very early age) strength and EMI indices of mortar is linearly correlated, as shown in most previous studies. The data points are all located within the 90% prediction band.

In conclusion, the feasibility of using piezoelectric sensor coupled with EMI method on monitoring the very early age strength of cementitious materials have been systematically studied via abundant experimental outcome. We have proved that this method is reliable for concrete strength monitoring regardless the type of cements and water/cement ratios. Nevertheless, several issue should be studied in the future to ensure the field implementations. For instance, the effect of ambient environments such as temperature and humidity on the test results should be studied. The cementitious mixes with different size of aggregate, supplementary cementitious materials (SCMs) etc. still need to be further studied. Once the issues mentioned above are addressed, the revolutionary non-destructive method for determine the quality of concrete will be established for in-situ application.

Declaration of Competing Interest

None.

Acknowledgements

This work is supported in part by the Joint Transportation Research Program (JTRP 4210) administered by the Indiana Department of Transportation and Purdue University, United States.

References

[1] E. Ghafari, Y. Yuan, C. Wu, T. Nantung, N. Lu, Evaluation the compressive strength of the cement paste blended with supplementary cementitious materials using a piezoelectric-based sensor, Constr. Build. Mater. 171 (2018) 504–510.
[2] H. Gu, G. Song, H. Dhonde, Y.L. Mo, S. Yan, Concrete early-age strength monitoring using embedded piezoelectric transducers, Smart Mater. Struct. 15 (6) (2006) 1837–1845.
[3] Y.-F. Su, R.R. Kotian, N. Lu, Energy harvesting potential of bendable concrete using polymer based piezoelectric generator, Compos. B Eng. 153 (2018) 124–129.
[4] G. Park, H. Sohn, C.R. Farrar, D.J. Inman, Overview of Piezoelectric Impedance-Based Health Monitoring and Path Forward, The Shock and Vibration Digest 35 (6) (2003) 13.
[5] C.K. Soh, S. Bhalla, Calibration of piezo-impedance transducers for strength prediction and damage assessment of concrete, Smart Mater. Struct. 14 (4) (2005) 671–684.
[6] S.W. Shin, A.R. Qureshi, J.Y. Lee, C.B. Yun, Piezoelectric sensor based nondestructive active monitoring of strength gain in concrete, Smart Mater. Struct. 17 (5) (2008).
[7] R. Tawie, H.K. Lee, Monitoring the strength development in concrete by EMI sensing technique, Constr. Build. Mater. 24 (9) (2010) 1746–1753.
[8] D. Wang, H. Zhu, Monitoring of the strength gain of concrete using embedded PZT impedance transducer, Constr. Build. Mater. 25 (9) (2011) 3703–3708.
[9] X. Lu, Y.Y. Lim, C.K. Soh, A novel electromechanical impedance–based model for strength development monitoring of cementitious materials, Struct. Health Monit. 17 (4) (2017) 902–918.
[10] P. Negi, T. Chakraborty, N. Kaur, S. Bhalla, Investigations on effectiveness of embedded PZT patches at varying orientations for monitoring concrete hydration using EMI technique, Constr. Build. Mater. 169 (2018) 489–498.
[11] R. Tawie, H.K. Lee, Piezoelectric-based non-destructive monitoring of hydration of reinforced concrete as an indicator of bond development at the steel–concrete interface, Cem. Concr. Res. 40 (2010) 7.
[12] Q. Kong, S. Hou, Q. Ji, Y.L. Mo, G. Song, Very early age concrete hydration characterization monitoring using piezoceramic based smart aggregates, Smart Mater. Struct. 22 (085025) (2013) 7.
[13] C.P. Providakis, E.V. Liarakos, E. Kampianakis, NondestructiveWirelessMonitoring of early-age concrete strength gain using

an innovative electromechanical impedance sensing system, Smart Mater. Res. 2013 (2013) 10.
[14] A. Narayanan, A. Kocherla, K.V.L. Subramaniam, Embedded PZT sensor for monitoring mechanical impedance of hydrating cementitious materials, J. Nondestr. Eval. 36 (64) (2017).
[15] T. Visalakshi, S. Bhalla, A. Gupta, Monitoring early hydration of reinforced concrete structures using structural parameters identified by piezo sensors via electromechanical impedance technique, Mech. Syst. Sig. Process. 99 (2018) 13.
[16] V.G.M. Annamdas, P. Rizzo, Monitoring Concrete by Means of Embedded Sensors and Electromechanical Impedance Technique, in: SPIE Smart Structures and Materials + Nondestructive Evaluation and Health Monitoring, SPIE, 2010, p. 8.
[17] J.-W. Kim, C. Lee, S. Park, K.-T.J.K.J.O.C.E. Koh, Real-time strength development monitoring for concrete structures using wired and wireless electro-mechanical impedance techniques, 17(6) (2013) 1432-1436.
[18] K. Qingzhao, H. Shuang, J. Qing, Y.L. Mo, S. Gangbing, Very early age concrete hydration characterization monitoring using piezoceramic based smart aggregates, Smart Mater. Struct. 22 (8) (2013) 085025.
[19] C.P. Providakis, E.V. Liarakos, E. Kampianakis, Nondestructive wireless monitoring of early-age concrete strength gain using an innovative electromechanical impedance sensing system %J, Smart Mater. Res 2013 (2013) 10.
[20] D.S. Wang, H.Y. Song, H.P. Zhu, Embedded 3D electromechanical impedance model for strength monitoring of concrete using a PZT transducer, Smart Mater. Struct. 23 (11) (2014).
[21] A. Narayanan, A. Kocherla, K.V.L. Subramaniam, Embedded PZT sensor for monitoring mechanical impedance of hydrating cementitious materials, J. Nondestruct. Eval. 36 (4) (2017).
[22] V. Talakokula, S. Bhalla, A. Gupta, Monitoring early hydration of reinforced concrete structures using structural parameters identified by piezo sensors via electromechanical impedance technique, Mech. Syst. Sig. Process. 99 (2018) 129–141.
[23] Y.-F. Su, A. Amran, T. Nantung, N.L. Lu, Systematically Investigation of Using Electromechanical Impedance (EMI) Technique for Monitoring the Very Early Age Properties of Cementitious Materials, The Transportation Research Board (TRB) 98th Annual Meeting, Transportation Research Board of the National Academies, Washington, DC, US, 2019.
[24] B.L. Grisso, D.J. Inman, Temperature corrected sensor diagnostics for impedancebased SHM, J. Sound Vib. 329 (12) (2010) 14.
[25] R. Tawie, H.K. Lee, Piezoelectric-based non-destructive monitoring of hydration of reinforced concrete as an indicator of bond development at the steel–concrete interface, Cem. Concr. Res. 40 (12) (2010) 1697–1703.
[26] D. Ai, H. Zhu, H. Luo, Sensitivity of embedded active PZT sensor for concrete structural impact damage detection, Constr. Build. Mater. 111 (2016) 348–357.
[27] V.G.M. Annamdas, M.A. Radhika, C.K. Soh, Health Monitoring of Concrete Structures using Embedded PZT Transducers based Electromechanical impedance Model, in: SPIE Smart Structures and Materials + Nondestructive Evaluation and Health Monitoring, SPIE, 2009, p. 9.
[28] V.G.M. Annamdas, P. Rizzo, Influence of the Excitation Frequency in the Electromechanical Impedance Method for SHM Applications, in: SPIE Smart Structures and Materials + Nondestructive Evaluation and Health Monitoring, SPIE, 2009, p. 11.
[29] N. Arun, V.L.S. Kolluru, Sensing of damage and substrate stress in concrete using electro-mechanical impedance measurements of bonded PZT patches, Smart Mater. Struct. 25 (9) (2016) 095011.
[30] F.G. Baptista, J.V. Filho, Optimal frequency range selection for PZT transducers in impedance-based SHM systems, IEEE Sens. J. 10 (8) (2010) 1297–1303.
[31] B.S. Divsholi, Y. Yang, Application of Reusable PZT Sensors for Monitoring Initial Hydration of Concrete, in: SPIE Smart Structures and Materials + Nondestructive Evaluation and Health Monitoring, SPIE, 2009, p. 9.
[32] A. Dixit, A. Bindal, S. Bhalla, Damage Prognosis of Plain Concrete Under Low-Cycle Fatigue Using Piezo-Based Concrete Vibration Sensors, Singapore Springer, Singapore, 2018, pp. 389–396.
[33] A. Narayanan, K.V.L. Subramaniam, Experimental evaluation of load-induced damage in concrete from distributed microcracks to localized cracking on electro-mechanical impedance response of bonded PZT, Constr. Build. Mater. 105 (2016) 536–544.
[34] H. Sohn, C. Farrar, D. Inman, Overview of Piezoelectric Impedance-Based Health Monitoring and Path Forward, 2003.
[35] S. Sung Woo, Q. Adeel Riaz, L. Jae-Yong, Y. Chung Bang, Piezoelectric sensor based nondestructive active monitoring of strength gain in concrete, Smart Mater. Struct. 17 (5) (2008) 055002.
[36] V. Talakokula, S. Bhalla, R.J. Ball, C.R. Bowen, G.L. Pesce, R. Kurchania, B. Bhattacharjee, A. Gupta, K. Paine, Diagnosis of carbonation induced corrosion initiation and progression in reinforced concrete structures using piezo-impedance transducers, Sens. Actuators, A 242 (2016) 79–91.
[37] D. Wang, J. Zhang, H. Zhu, Embedded electromechanical impedance and strain sensors for health monitoring of a concrete bridge %J, Shock Vib. (2015) 12.
[38] Y. Yang, Y. Hu, Y. Lu, Sensitivity of PZT Impedance Sensors for Damage Detection of Concrete Structures, 8(1) (2008) 327.
[39] F.G.B. Baptista, J.V. Filho, Optimal frequency range selection for PZT transducers in impedance-based SHM systems, IEEE Sens. J. 10 (8) (2010).
[40] Z. Guo, Z. Sun, Piezoelectric Impedance-based Strength Gain Monitoring in Concrete, Sensors and Smart Structures Technologies for Civil, Mechanical, and Aerospace Systems 2012, SPIE - The International Society for Optical Engineering, USA, 2012, pp. 12834524–12834615. 8 pp.